R. Mahalakshmi
A. Sengupta
S. Raghothama
N. Shamala
P. Balaram

Tryptophan-containing peptide helices: interactions involving the indole side chain*

Authors' affiliations:
P. Balaram and R. Mahalakshmi, Molecular Biophysics Unit, Indian Institute of Science, Bangalore 560012, India

N. Shamala and A. Sengupta, Department of Physics, Indian Institute of Science, Bangalore 560012, India

S. Raghothama, NMR Research Center, Indian Institute of Science, Bangalore 560012, India

Correspondence to:
P. Balaram
Molecular Biophysics Unit
Indian Institute of Science
Bangalore 560012
India
Tel.: 91-80-22932337
Fax: 91-80-23600535
E-mail: pb@mbu.iisc.ernet.in

Dates:
Received 23 July 2005
Accepted 29 August 2005

*Dedicated to Victor J. Hruby on his 65th birthday.

To cite this article:
Mahalakshmi, R., Sengupta, A., Raghothama, S.R., Shamala, N. & Balaram, P. Tryptophan-containing peptide helices: interactions involving the indole side chain.
J. Peptide Res., 2005, **66**, 277–296.
DOI 10.1111/j.1399-3011.2005.00301.x

Key words: aromatic interactions; C-H…π interactions; indole NH hydrogen bonding; nuclear magnetic resonance structures; peptide aggregation; tryptophan peptides

Abstract: Two designed peptide sequences containing Trp residues at positions *i* and *i* + 5 (Boc-Leu-Trp-Val-Ala-Aib-Leu-Trp-Val-OMe, **1**) as well as *i* and *i* + 6 (Boc-Leu-Trp-Val-Aib-Ala-Aib-Leu-Trp-Val-OMe, **2**) containing one and two centrally positioned Aib residues, respectively, for helix nucleation, have been shown to form stable helices in chloroform solutions. Structures derived from nuclear magnetic resonance (NMR) data reveal six and seven intramolecularly hydrogen-bonded NH groups in peptides **1** and **2**, respectively. The helical conformation of octapeptide **1** has also been established in the solid state by X-ray diffraction. The crystal structure reveals an interesting packing motif in which helical columns are stabilized by side chain–backbone hydrogen bonding involving the indole Nε1H of Trp(2) as donor, and an acceptor C=O group from Leu(6) of a neighboring molecule. Helical columns also associate laterally, and strong interactions are observed between the Trp(2) and Trp(7) residues on neighboring molecules. The edge-to-face aromatic interactions between the indoles suggest a potential C-H…π interaction involving the Cζ3H of Trp(2). Concentration dependence of NMR chemical shifts provides evidence for peptide association in solution involving the Trp(2) Nε1H protons, presumably in a manner similar to that observed in the crystal.

Abbreviations: NOE, Nuclear Overhauser effect; RMSD, root mean square deviation; ROESY, rotating frame nuclear Overhauser enhancement and exchange spectroscopy; TOCSY, total correlation spectroscopy; TPPI, time proportional phase incrementation.

Introduction

Aromatic interactions contribute to protein and DNA stability (1–6), form recognition motifs in proteins and enzymes (7,8), and are of recent interest in the study of amyloidogenesis (9,10). Of the aromatic residues, the side chain of tryptophan (Trp) is unique, with its amphipathic nature enabling it to participate in both nonpolar interactions and in hydrogen bonding (11–14). NH…π (15–17) and CH…π interactions (18) and electrostatic interactions via the inherent quadrupoles of the aromatic ring (12,19,20) also make the Trp residue an important contributor, both to

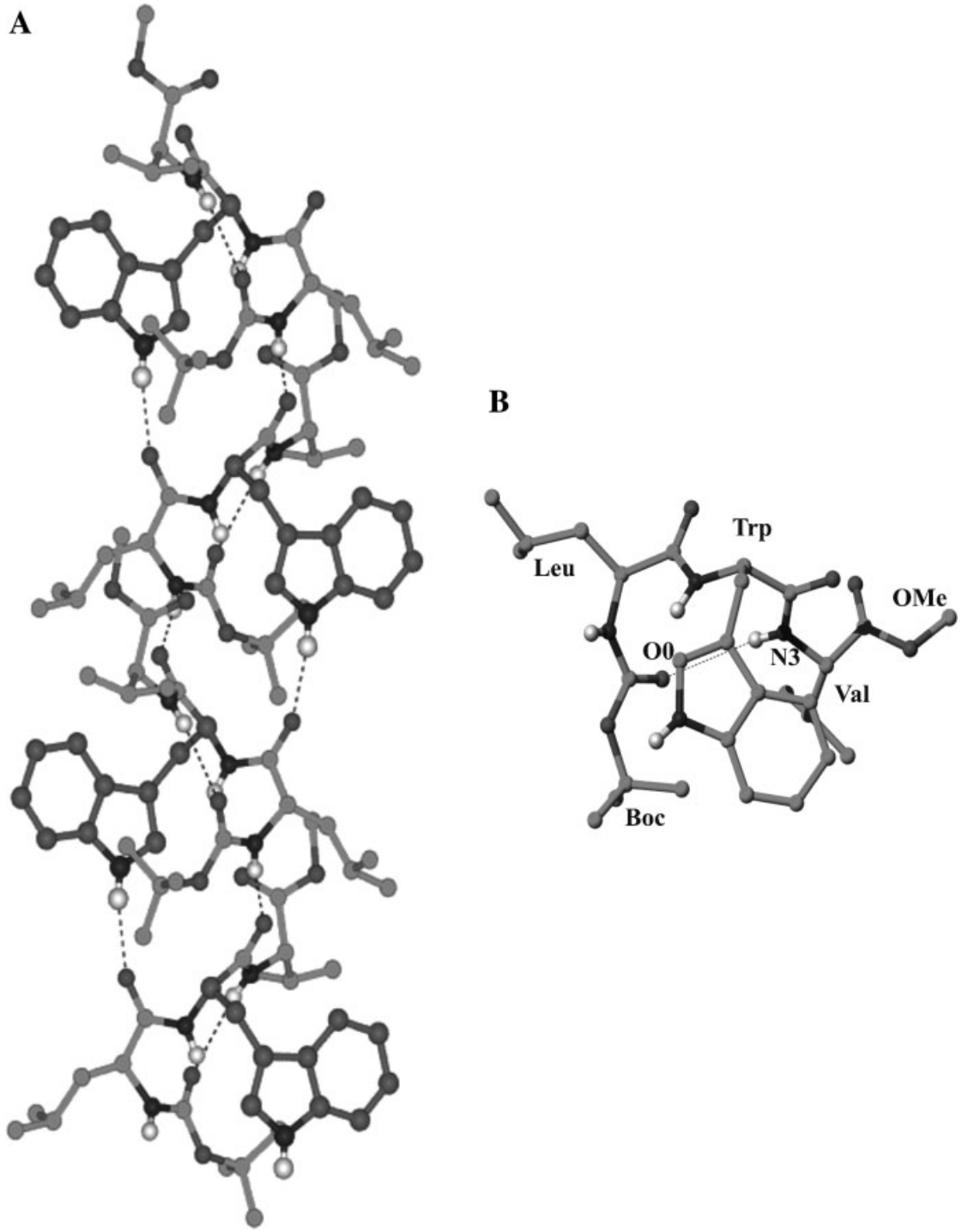

Figure 1. (A) View of superhelical column of Boc-Leu-Trp-Val-OMe, **4**. Hydrogen bonds are indicated by dotted lines; (B) molecular conformation of peptide **4** in crystals. The intramolecular hydrogen bond is shown.

the process of protein folding and subsequent stabilization of the folded structures. For example, the role of Trp residues in stabilizing tertiary structure, leading to alternate folding patterns of proteins, has been emphasized in a recent study of a 20-residue peptide (21). A recent study of hen lysozyme has clearly demonstrated the importance of Trp residues in the formation of hydrophobic clusters (22). These properties of the indole ring have been exploited in the design of a highly stable peptide β-hairpin with protein-like properties (23). The amphipathic nature of Trp residues is also of great advantage in stabilizing membrane proteins, wherein it is predominantly found to occur at the lipid–water interface (24–26). A classical example of Trp residues in membranes is that of the gramicidin channel, wherein the dipole moment of the indole ring appears to affects channel conductance (27–30). Additionally, Trp residues are also useful for the study of protein dynamics and structural changes with ligand binding, as the fluorescence properties of the indole are highly environment-sensitive (31). Analysis of Trp residues has however, been largely limited to the available protein crystal structures (14,32,33) and relatively little information on the interactions of Trp residues in peptide structures is available. A search of the Cambridge Structural Database (CSD) (34) revealed only 31 examples of crystal structures of Trp-containing peptides. As a part of a program designed to study Trp-rich peptides, we encountered the formation of an unusual supramolecular helix in the crystal structure of the tripeptide Boc-Leu-Trp-Val-OMe (Fig. 1A) (35). A key feature of the conformation of the peptide (Fig. 1B), is the intermolecular hydrogen bond formed by the Trp(2) indole N-H of molecule 1 to the C=O of Leu(1) in molecule 2. Curiously, the acetyl derivative yielded a completely different conformation, an extended β-sheet structure (35). The observation of an intermolecular backbone–side chain hydrogen bond in the superhelical assembly prompted us to examine longer sequences in which two -Leu-Trp-Val- tripeptide segments were covalently connected by linking dipeptide and tripeptide segments. We have used the linking segments Ala-Aib and Aib-Ala-Aib because of the known tendency of Aib residues to promote helix formation in short peptides (36). The octapeptide Boc-Leu-Trp-Val-Ala-Aib-Leu-Trp-Val-OMe (peptide **1**) and nonapeptide Boc-Leu-Trp-Val-Aib-Ala-Aib-Leu-Trp-Val-OMe (peptide **2**) are shown to form stable helical structures in chloroform solution as determined by nuclear magnetic resonance (NMR). In addition, the 8-residue peptide adopts a helical conformation in crystals. The Trp residues are extended away from the helical backbone in both solution and in the solid state. An intermolecular hydrogen bond between the indole N-H of one helix and Leu C=O of the neighboring molecule in the crystal is observed for peptide **1**, which closely resembles the hydrogen-bonding pattern obtained in the tripeptide Boc-Leu-Trp-Val-OMe, stabilizing a head-to-tail arrangement of helices into columns. The crystal structure also revealed an example of a 'free', nonhydrogen bonded indole NH and a T-shaped arrangement of facing Trp residues in the solid state.

Table 1. **Crystal and diffraction parameters for peptide 1 Boc-Leu-Trp-Val-Ala-Aib-Leu-Trp-Val-OMe**

Empirical formula	$C_{57}H_{84}N_{10}O_{11}$
Crystal habit	Small plate
Crystal size (mm)	0.21 × 0.12 × 0.03
Crystallizing solvent	Ethanol/water
Space group	P1
Temperature (°C)	20
Cell parameters	
a (Å)	10.494(7)
b (Å)	11.989(7)
c (Å)	13.834(9)
α (°)	70.100(9)
β (°)	82.744(10)
γ (°)	78.959(10)
Volume (Å^3)	1602.7(17)
Z	1
Molecules/asymmetric unit	1
Co-crystallized solvent	None
Molecular weight	1085.34
Density (g/cm^3; cal)	1.124
F(000)	584
Radiation (Å)	MoKα (λ = 0.71073 Å)
2θ maximum (°)	46.52
Scan type	ω scan
Measured reflections	12782
Independent reflections	9011
Unique reflections	4586
Observed reflections [|Fo| > 4σ(Fo)]	2446
R_{int}	0.055
Goodness-of-fit (S)	1.036
$\Delta\rho_{max}$ (eÅ^{-3})	0.536
$\Delta\rho_{min}$ (eÅ^{-3})	−0.230
Final *R* (%)	8.53
Final R_w (%)	19.62
Number of restraints/parameters	14/691
Data-to-parameter ratio	3.54 : 1

Experimental Section

Peptide synthesis

Peptides **1** and **2** were synthesized by conventional solution phase methods using a fragment condensation strategy (37). *t*-butyloxycarbonyl (Boc) and methoxy (OMe) groups were used as the N- and C-terminal protecting groups, respectively. Deprotection of the Boc group was achieved using 98–100% formic acid and the methyl ester was saponified using methanolic NaOH. Trp residues were used without side chain protection. Coupling reactions were mediated by dicyclohexyl carbodiimide/hydroxybenzotriazole (DCC/HOBt). Some of the intermediates were characterized by thin layer chromatography (TLC) on a silica gel and 80 MHz ^{1}H-NMR spectroscopy, and used without further purification. The final peptides were purified on a reverse phase medium pressure liquid chromatography column (MPLC; C_{18}, 40–60 μ) using methanol–water gradients. The mass spectra of the peptides were recorded on a Kompaq SEQ MALDI-TOF mass spectrometer (Kratos Analytical, Manchester, UK). Peptide **1**: $M^+_{Na} = 1108.6$ Da, $M^+_K = 1124.5$ Da, $M_{cal} = 1084.0$ Da; Peptide **2**: $M^+_{Na} = 1193.7$ Da, $M^+_K = 1209.8$ Da, $M_{cal} = 1169.0$ Da. All target peptides were fully characterized by 500 MHz NMR spectroscopy.

NMR

NMR data acquisition

All NMR experiments were carried out on a Bruker DRX-500 (Bruker Biospin, Switzerland) spectrometer.

Table 2. **^{1}H-NMR parameters for peptides 1 (top) and 2 (bottom) in $CDCl_3$ at 500 MHz and 300 K**

Residue	NH (p.p.m.)	$C^\alpha H$ (p.p.m.)	$C^\beta H$ (p.p.m.)	$C^\gamma H$ (p.p.m.)	Others (p.p.m.)	$^3J_{NH\text{-}C^\alpha H}$ (Hz)
Peptide **1**						
Leu(1)	5.21	3.82	1.65	1.42	$C^\delta H$: 0.90	2.7
			1.54			
Trp(2)	7.01	4.42	3.34	–	$C^{\delta 1}H$: 7.12, $N^{\varepsilon 1}H$: 8.74, $C^{\varepsilon 3}H$: 7.53, $C^{\zeta 2}H$: 7.40, $C^{\zeta 3}H$: 7.15, $C^{\eta 2}H$: 7.22	4.7
Val(3)	6.89	3.88	1.95	0.83	–	5.9
Ala(4)	7.24	3.66	1.31	–	–	–
Aib(5)	7.26	–	1.58	–	–	–
Leu(6)	7.26	4.28	1.81	1.68	$C^\delta H$: 0.98, 0.93	–
Trp(7)	7.79	4.79	3.61	–	$C^{\delta 1}H$: 7.26, $N^{\varepsilon 1}H$: 7.98, $C^{\varepsilon 3}H$: 7.69, $C^{\zeta 2}H$: 7.32, $C^{\zeta 3}H$: 7.06, $C^{\eta 2}H$: 7.10	8.4
			3.29			
Val(8)	7.31	4.49	2.26	1.03	–	5.6
Peptide **2**						
Leu(1)	5.07	3.83	1.67	1.43	$C^\delta H$: 0.92	~1
			1.56			
Trp(2)	6.97	4.40	3.34	–	$C^{\delta 1}H$: 7.12, $N^{\varepsilon 1}H$: 8.64, $C^{\varepsilon 3}H$: 7.55, $C^{\zeta 2}H$: 7.41, $C^{\zeta 3}H$: 7.18, $C^{\eta 2}H$: 7.25	4.3
Val(3)	6.97	3.83	1.95	0.85	–	5.2
Aib(4)	7.18	–	1.50	–	–	–
			1.46			
Ala(5)	7.36	3.69	1.42	–	–	5.6
Aib(6)	7.78	–	1.06	–	–	–
			1.56			
Leu(7)	7.33	4.30	1.75	1.68	$C^\delta H$: 0.95, 0.93	6.7
Trp(8)	7.91	4.78	3.63	–	$C^{\delta 1}H$: 7.25, $N^{\varepsilon 1}H$: 8.05, $C^{\varepsilon 3}H$: 7.71, $C^{\zeta 2}H$: 7.29, $C^{\zeta 3}H$: 7.07, $C^{\eta 2}H$: 7.13	8.3
			3.29			
Val(9)	7.38	4.48	2.27	1.05	–	8.5
				1.03		

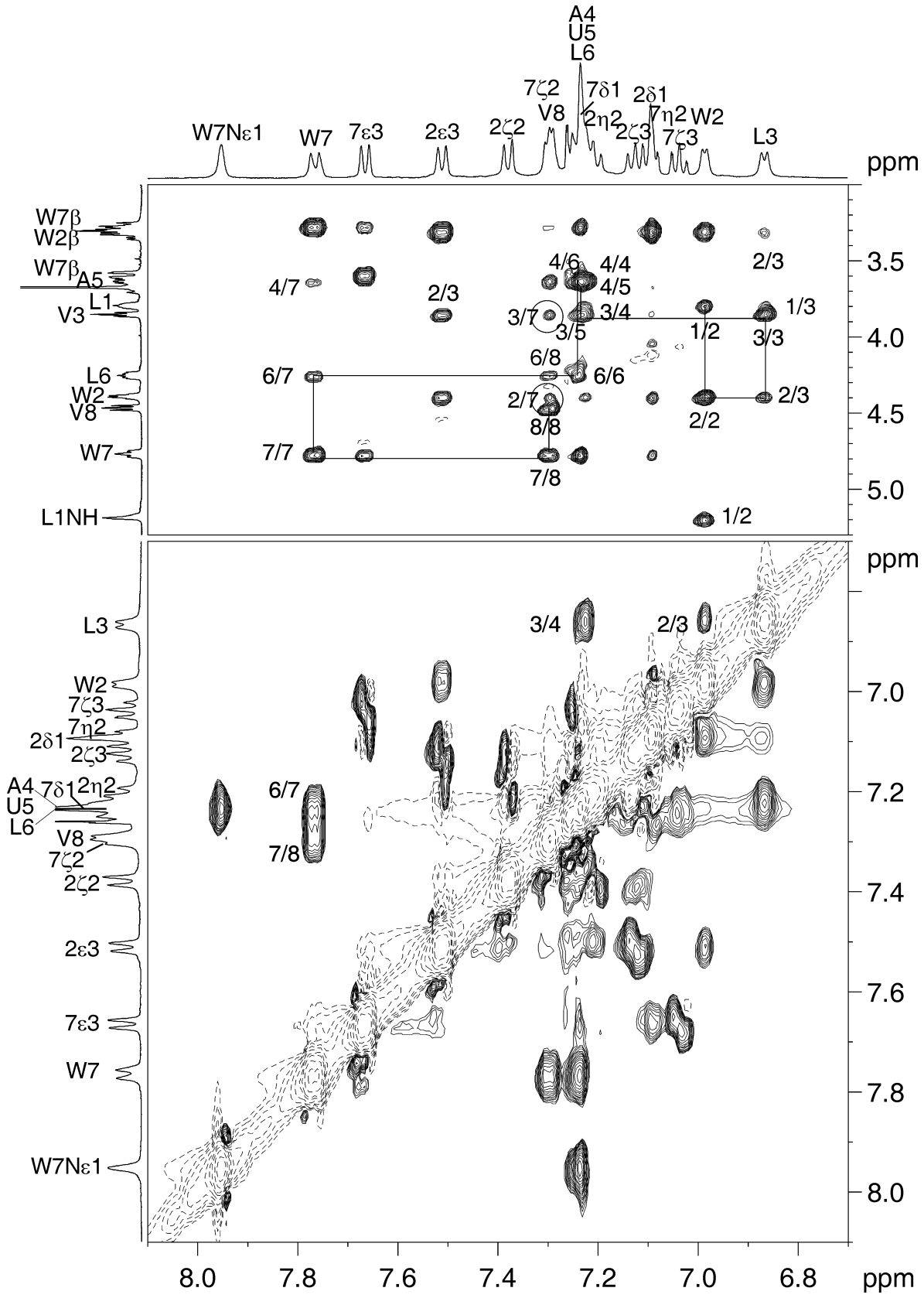

Figure 2. Partial expansions of the ROESY spectrum of peptide **1** in $CDCl_3$ at 300 K. $d_{N\alpha/\beta}$ (top) and d_{NN} (bottom) NOEs are annotated.

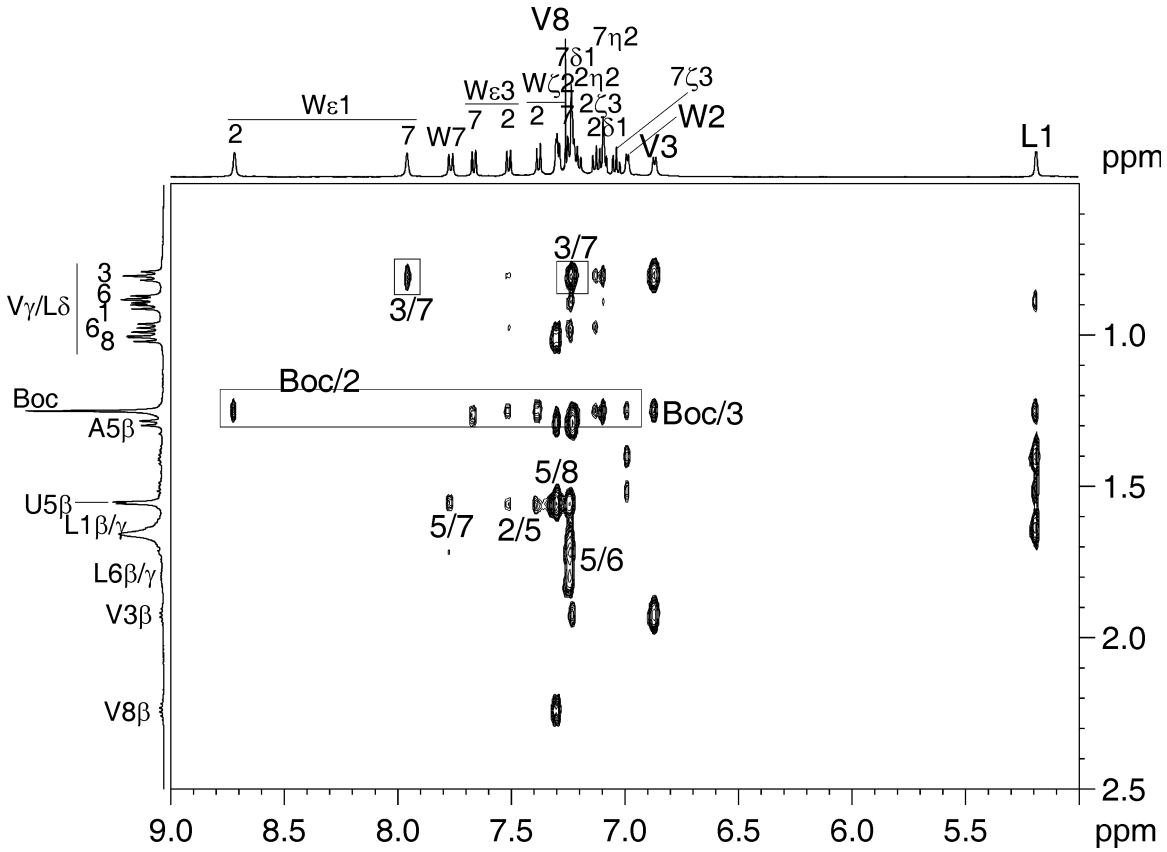

Figure 3. Partial expansion of the ROESY spectrum of peptide **1**. NOEs obtained between the aromatic ring protons and the N-terminal protecting group (Boc) for peptide **1** are boxed.

Peptide concentrations of approximately 10 mM in $CDCl_3$ were used for collecting NMR data for structure determination. Peptide aggregation was studied by comparing the backbone chemical shifts in chloroform at concentrations ranging from 10 to 0.1 mg/mL. Complete assignment of the one-dimensional (1D) spectrum was achieved using a combination of total correlation spectroscopy (TOCSY) (38) and rotating frame nuclear Overhauser enhancement and exchange spectroscopy (ROESY) (39,40) experiments. All two-dimensional (2D) experiments were recorded in the phase-sensitive mode using time proportional phase incrementation (TPPI) method. About 1024 data points were collected in the f2 dimension and 512 data points in the f1 dimension. NMR data were processed using the Bruker XWINNMR software on a Silicon Graphics Indy workstation. The data were zero-filled to 2 K points in the f1 dimension and a shifted ($\pi/2$) sine-squared window function was applied to both the dimensions, prior to Fourier transformation. Hydrogen-bonding information was obtained from $CDCl_3$-dimethyl sulfoxide (DMSO) titration experiments (41–43).

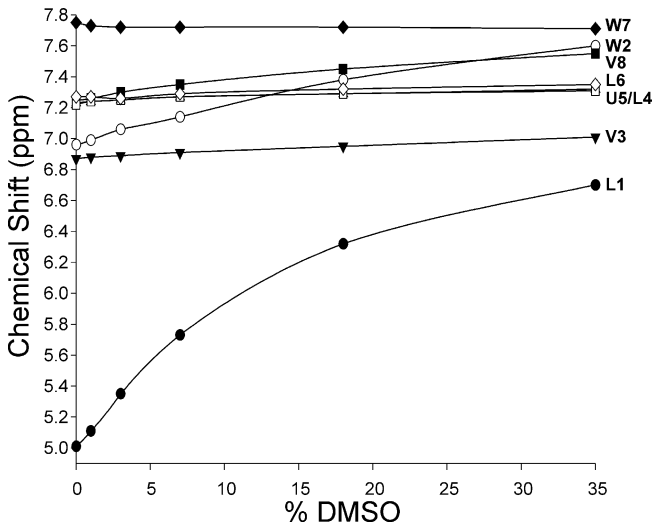

Figure 4. Plot of the chemical shift variation of backbone amide resonances of peptide **1** in $CDCl_3$ as a function of added dimethyl sulfoxide (DMSO) concentration. Note the large variation seen in residues 1 and 2 (peptide concentration: 10 mg/mL).

Structure calculation

The Nuclear Overhauser effects (NOEs) were classified as strong (2.0–2.5 Å), medium (2.5–3.5 Å), and weak (3.5–5.0 Å) by visual inspection. Structure calculation was performed using DYANA v1.5 (44). A total of 119 NOEs (56 self, 37 sequential, 26 long range) were used for peptide **1**.

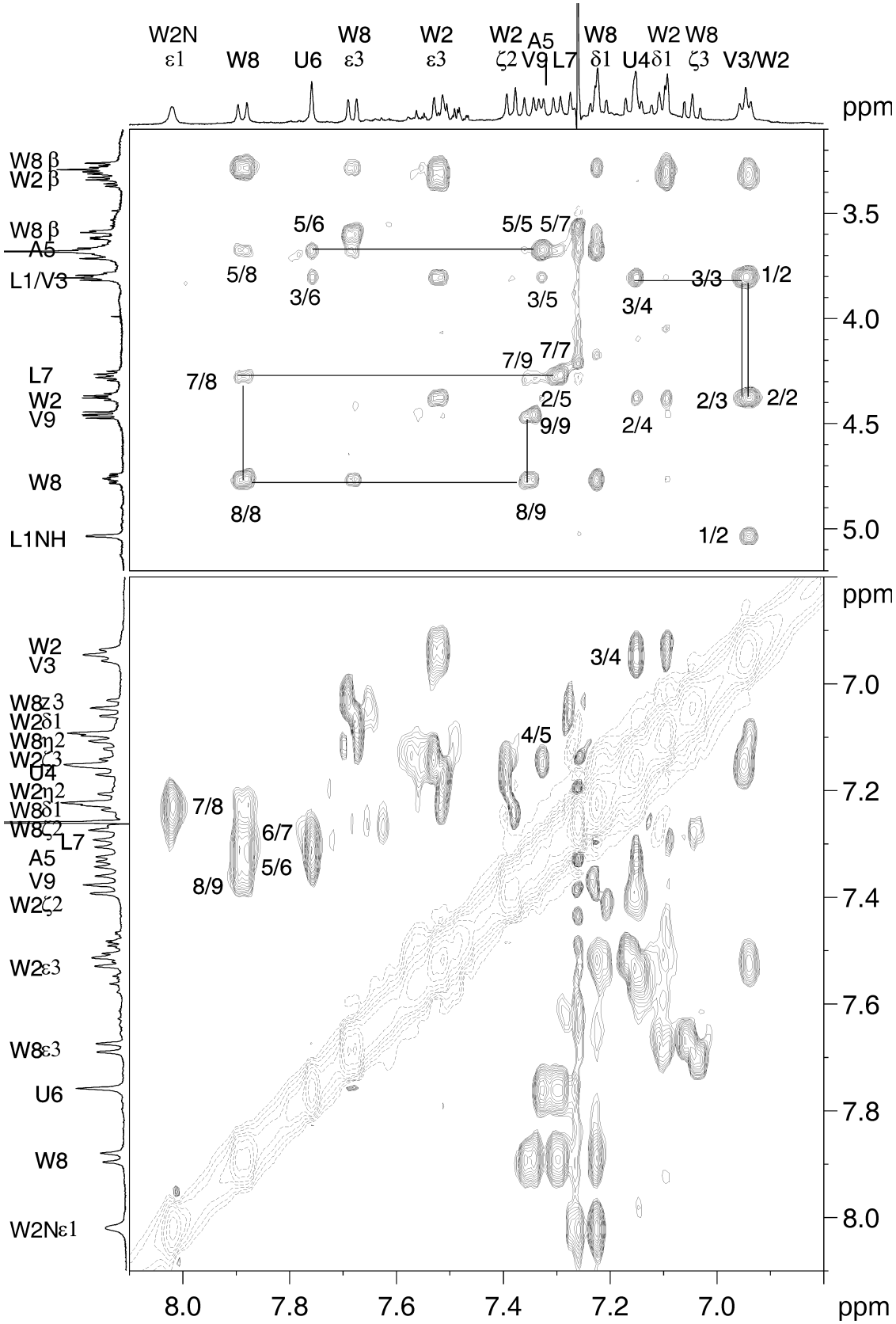

Figure 5. Partial expansions of the ROESY spectrum of peptide **2** in $CDCl_3$ at 300 K. $d_{N\alpha/\beta}$ (top) and d_{NN} (bottom) NOEs are annotated.

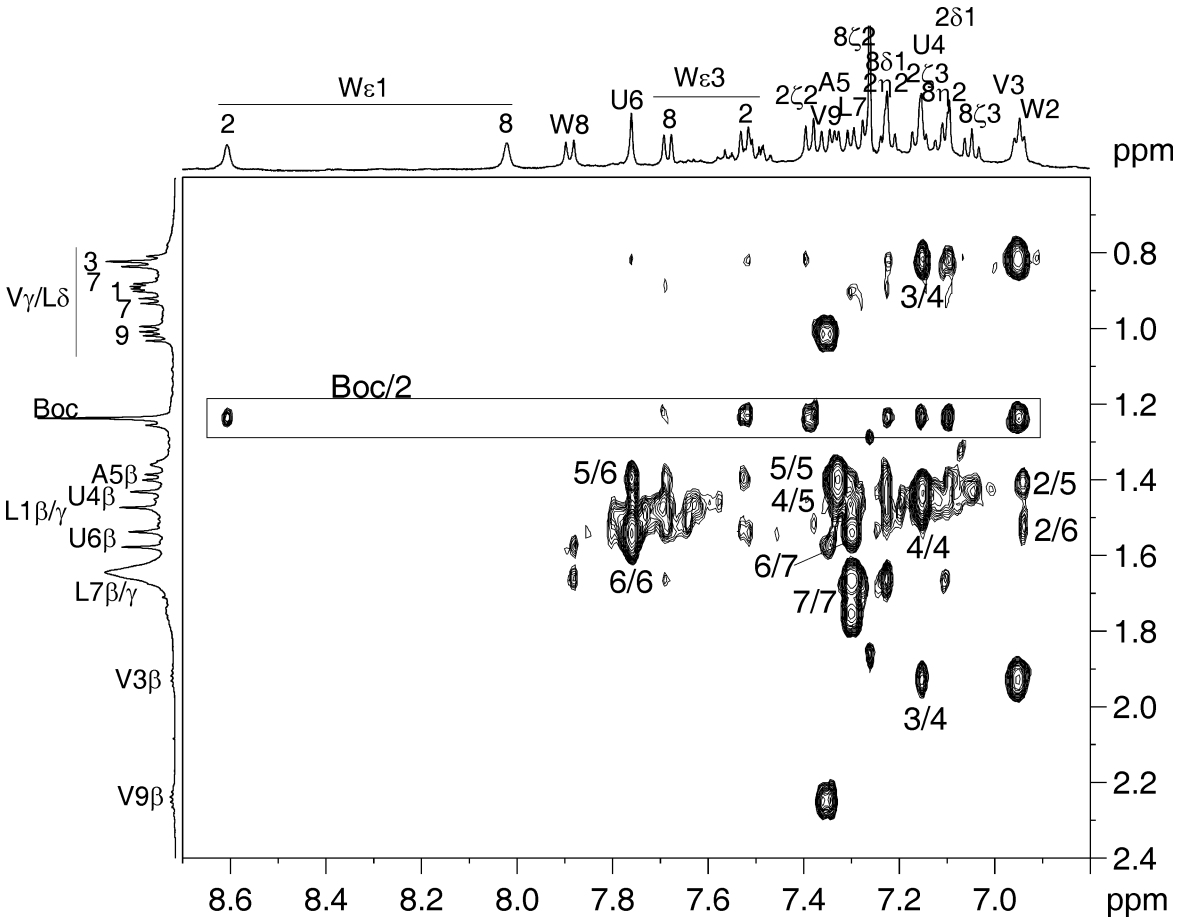

Figure 6. Partial expansion of the ROESY spectrum of peptide **1**. NOEs obtained between the aromatic ring protons and the N-terminal protecting group (Boc) in peptide **2** are boxed.

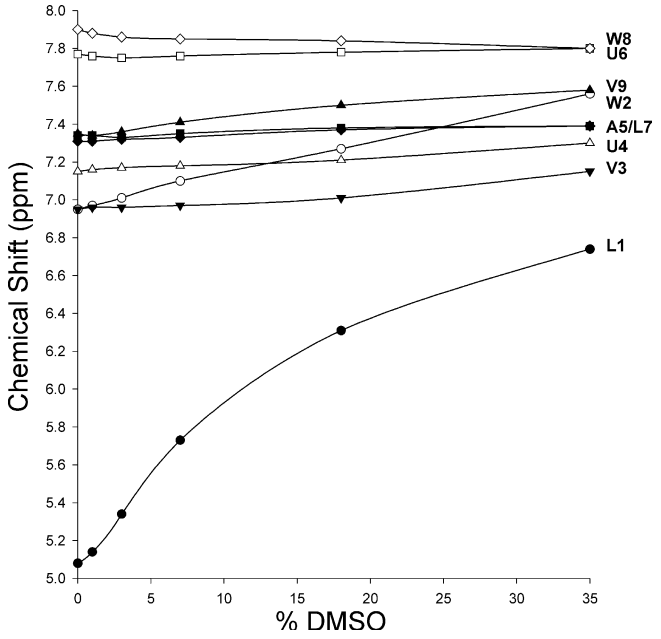

Figure 7. Chemical shift variation of backbone NH resonances in peptide **2**, in $CDCl_3$, with increasing dimethyl sulfoxide (DMSO) concentration. The amide resonances of residues 1 and 2 show a strong solvent dependence (peptide concentration: 10 mg/mL).

The structures were refined using nine angle constraints (ϕ constraints for each residue was obtained from the $^3J_{N\alpha}$ coupling constants, ϕ and ψ constraints were used for Aib5) and five hydrogen-bonding constraints obtained from DMSO titration experiments. For peptide **2**, 89 NOEs (59 self, 23 sequential, seven long range) were used. Structure refinement was carried out using 11 angle constraints (ϕ constraints for each residue was obtained from the $^3J_{N\alpha}$ coupling constants, ϕ and ψ constraints were used for Aib4 and Aib6) and six hydrogen-bonding constraints. Structures were refined until there were no violated constraints and short contacts. The calculated 50 structures were superposed using MOLMOL (45). Backbone torsion angles were calculated for three selected structures and compared with that obtained in the mean structure.

X-ray diffraction

Single crystals of peptide **1** suitable for X-ray diffraction, were grown from ethanol/water mixtures by slow evapor-

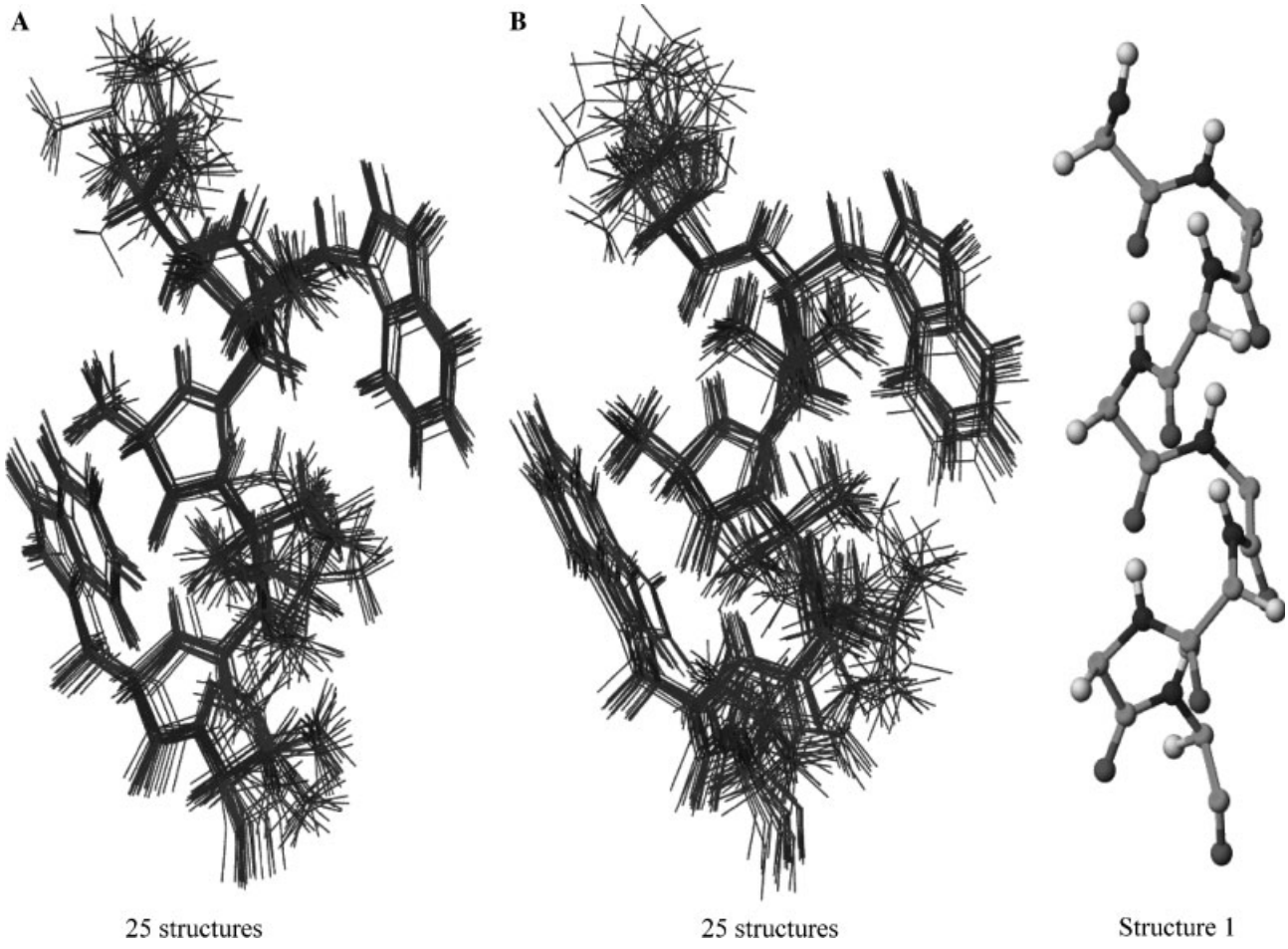

Figure 8. Superposition of calculated solution structures for peptide **1**. The two sets of calculated solution structures differ in the orientation of the indole ring of Trp(7). (A) 25 structures (mean global heavy atom RMSD: 0.76 ± 0.21 Å) and (B) 25 structures (mean global heavy atom RMSD: 0.73 ± 0.17 Å), respectively. The mean structure obtained for the peptide (all 50 structures; backbone atoms only) is represented in a ball-and-stick form.

ation. X-ray intensity data were collected at room temperature on a Bruker AXS (Madison, WI, USA) SMART APEX CCD diffractometer using MoK_α radiation ($\lambda = 0.71073$ Å). The ω-scan type was used. The structure was solved by direct phase determination using SHELXD (46). About 65 atoms of 78 could be located from the electron density map while the rest were obtained from the difference Fourier map. The structure thus obtained was refined against F^2 by the full matrix least-squares method using the program SHELXL-97 (47). In the crystallographic refinement procedure restraints were applied on bond lengths and bond angles of 5-membered ring of indole (Cγ-Cδ1, Cδ1-Nε1, Nε1-Cε2, Cγ-Cδ2, ∠Cγ-Cδ1-Nε1, ∠Cδ1-Nε1-Cε2, ∠Nε1-Cε2-Cδ2, ∠Cγ-Cδ2-Cε2, ∠Cδ1-Cγ-Cδ2) and the C-C bond lengths of the 6-membered ring were restrained to 1.39 Å in Trp(7). At the end of the isotropic refinement, *R*-factor was 24.41%, which dropped to 15.16% after the anisotropic refinement was performed. The hydrogen atoms were all fixed geometrically into idealized positions and were refined in the final cycle of refinement as riding over the atoms to which they were bonded. After the final refinement, *R*-factor was 8.53% ($R_w = 19.62\%$) for 2446 observed reflections with $|Fo| \geq 4\sigma(Fo)$ for 691 variables. The relevant crystallographic data collection parameters and the details of the structure refinement are summarized in Table 1. CCDC-278382 (peptide **1**) contains the supplementary crystallographic data for this paper. This data can be obtained free of charge via http://www.ccdc.cam.ac.uk/products/csd/request or from the Cambridge Crystallographic Data Center, 12 Union Road, Cambridge $CB_{21}EZ$, UK [Fax: (+44) 1223-336-033] or by e-mail to deposit@ccdc.cam.ac.uk.

Results and Discussion

Solution NMR studies of peptides 1 and 2

Both peptides examined were highly soluble in nonpolar organic solvents. All 2D NMR experiments were therefore

Table 3. **Backbone torsion angles (in °) in nuclear magnetic resonance (NMR)-derived structures obtained for peptide 1[a]**

Number	Residue	Angle	Mol 1	Mol 25	Mol 50	Mean
1	Leu	ψ	−34.8	−35.0	−24.7	−33.6
2	Trp	ω	−180.0	180.0	−180.0	180.0
2	Trp	ϕ	−65.0	−65.0	−65.0	−65.0
2	Trp	ψ	−30.3	−32.7	−28.7	−30.9
3	Val	ω	−180.0	−180.0	−180.0	180.0
3	Val	ϕ	−54.8	−56.2	−55.9	−55.4
3	Val	ψ	−25.0	−25.0	−25.0	−25.0
4	Val	ω	180.0	180.0	−179.9	−180.0
4	Ala	ϕ	−59.9	−60.8	−61.0	−60.4
4	Ala	ψ	−29.3	−24.9	−25.1	−26.8
5	Aib	ω	175.8	175.8	175.8	175.9
5	Aib	ϕ	−54.9	−55.4	−55.8	−57.1
5	Aib	ψ	−27.1	−26.7	−26.3	−26.8
6	Leu	ω	180.0	179.2	−180.0	−180.0
6	Leu	ϕ	−65.0	−55.7	−55.9	−61.2
6	Leu	ψ	−35.1	−26.7	−26.5	−27.9
7	Trp	ω	−180.0	180.0	180.0	180.0
7	Trp	ϕ	−56.8	−54.9	−54.9	−57.3
7	Trp	ψ	−26.7	−35.0	−34.8	−30.7
8	Val	ω	180.0	−180.0	180.0	−180.0
8	Val	ϕ	−55.0	−56.9	−63.1	−59.7

a. Mol 1, Mol 25 and Mol 50 correspond to structures 1, 25 and 50 of the 50 calculated NMR structures, respectively.

carried out in $CDCl_3$ (10 mM at 300 K). A combination of TOCSY and ROESY experiments were used for complete assignment of all resonances. The ^{1}H-NMR parameters for peptides **1** and **2** are listed in Table 2. Exposed and hydrogen-bonded amide groups were identified by titrating the peptide in $CDCl_3$ against DMSO-d_6, maintaining constant peptide concentration. Secondary structure information was derived from sequential d_{NN} and long-range ($i - i + 2$ and $i - i + 3$) $d_{\alpha N}$ NOEs.

Backbone conformations of peptide 1

The ^{1}H 1D spectrum obtained for peptide **1** in $CDCl_3$ at 300 K was characterized by well-dispersed resonances, indicative of a well-folded structure. The backbone conformation of peptide **1** was inferred from the observed NOEs between backbone NH and $C^{\alpha}H$ protons and the values of $^3J_{HN\text{-}C^{\alpha}H}$ coupling constants. Figures 2 and 3 illustrate the observed NOEs for peptide **1**. Strong d_{NN} NOEs were obtained for all residues except for $d_{4N\text{-}5N}$ and $d_{5N\text{-}6N}$, which were lost because of resonance overlap. In addition, strong self-$d_{N\alpha}$ NOEs and weak sequential $d_{\alpha N}$ NOEs were observed, indicating that the peptide adopted a helical scaffold. Long-range $d_{\alpha N}$ NOEs ($i - i + 2$ and $i - i + 3$) that were present included 1α-3/4N, 3α-5/6N, 4α-6/7N, 5β-7/8N, 6α-8N. Peptide **1** showed marked changes in chemical shifts upon addition of DMSO to a $CDCl_3$ solution, for the amide resonances of residues Leu(1) and Trp(2), indicating that they are solvent exposed (Fig. 4). The amide resonances of residues 3–8 were largely invariant with increasing DMSO concentrations, suggesting that they were involved in strong internal hydrogen bonds. This feature is characteristic of a helical scaffold, wherein the first two or three NH groups are solvent exposed and show chemical shift variation with increasing concentrations of a strong hydrogen bonding solvent-like DMSO.

Backbone conformations of peptide 2

In the case of peptide **2**, a 3-residue linker was used between the two Leu-Trp-Val segments. This peptide also showed a well-dispersed NMR spectrum in chloroform, suggesting that the peptide was well folded. In the ROESY spectrum of the peptide, all sequential d_{NN} NOEs were observable, with the only exception of $d_{2N\text{-}3N}$, which was not observed due to resonance overlap (Figs 5 and 6). Additionally, strong self-$d_{N\alpha}$ NOEs and weak sequential $d_{\alpha N}$ NOEs were obtained. Long-range ($i - i + 2$ and $i - i + 3$) $d_{\alpha N}$ NOEs were also present, for example, 2α-4/5N, 3α-5/6N, 5α-7/8N, 6β-8N, 7α-9N. These NOEs clearly supported a well-folded helical scaffold for peptide **2**. In the DMSO titration experiment of peptide **2**, only Leu(1) and Trp(2) showed strong solvent dependence (Fig. 7), as was obtained for peptide **1**. This immediately suggested that all the amide resonances with the exception of 1 and 2, were involved in strong internal hydrogen bonds, a feature characteristic of a helix. It should be noted that in an α-helical structure, three N-terminal amide groups are solvent exposed, while in a 3_{10}-helix, two NH groups are exposed. However, a distinction between 3_{10}-and α-helices is not possible solely on the basis of the number of solvent exposed NH resonances. This is because mixed helical structures, which involve bifurcated hydrogen bonds in which a single carbonyl group acts as an acceptor for both $4 \rightarrow 1$ and $5 \rightarrow 1$ hydrogen bonds, are often observed at the N-terminal of helical peptides in the solid state (48). The persistence of such structures in solution renders distinction between 3_{10}- and α-helices ambiguous. In both peptides **1** and **2**, the indole side chain of the Trp residues can, in principle, also contribute to solvent shielding of adjacent amide NH resonances.

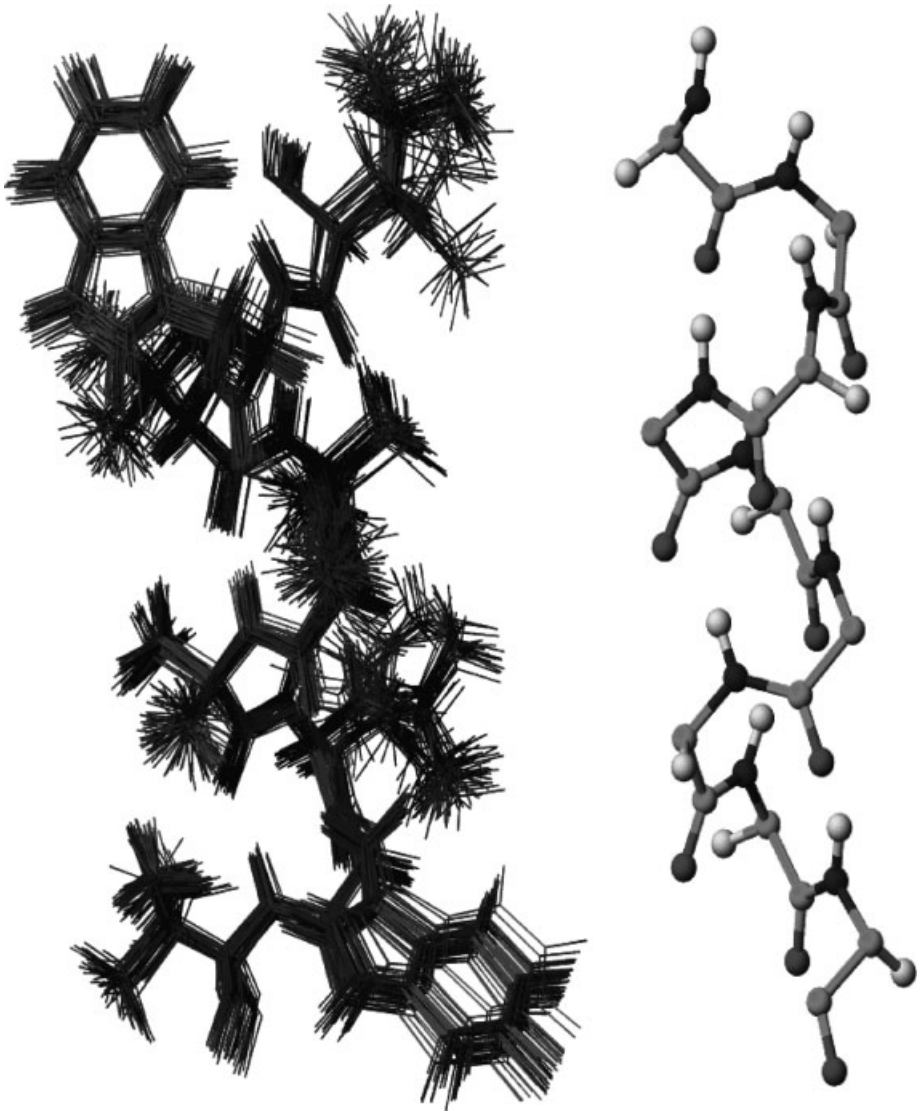

Figure 9. Superposition of 50 structures of peptide **2** calculated using DYANA (mean global heavy atom RMSD: 0.82 ± 0.22 Å). Mean structure (backbone atoms only) obtained is indicated as ball-and-stick.

NMR-derived structures of peptides 1 and 2 in chloroform

Peptide **1** gave an unusually large number of NOEs (37 sequential and 26 long range) for an 8-residue sequence, which permitted structure calculation using DYANA v1.5 (see Figs 2 and 3 for representative data). A total of 119 NOEs were employed to derive the solution structure. Figure 8 illustrates the calculated structure for peptide **1**. The calculated structure showed two conformations of the Trp(7), which differed in the orientation of the indole ring. NOEs were obtained in the ROESY spectrum supporting both the ring conformations. This observation is not surprising, as conformational flexibility is anticipated in solution, wherein strong interactions impeding side chain dynamics, are absent. The Trp(2) indole ring protons gave NOEs to the N-terminal protecting group (Boc), illustrated in Fig. 3. These NOEs were not be used in structure calculation, as protecting groups are unavailable in the DYANA v1.5 library. The mean global backbone root mean square deviation (RMSD) for the 50 structures calculated is 0.22 ± 0.13 Å and the mean global heavy atom RMSD is 1.08 ± 0.35 Å. A comparison of the torsion angles for three arbitrarily chosen NMR-derived conformations (structure 1, 25 and 50) were found to be very similar and the torsional angles are listed in Table 3.

In the case of peptide **2**, 89 NOEs were used in the structure calculation (see Figs 5 and 6 for representative data). Clear NOEs were obtained between the Boc group and the indole ring of Trp(2) (Fig. 6). Here again, these NOEs were not included during structure calculation. Ring positions were derived, instead, from NOEs obtained between Trp(2) and the backbone and side chain of Leu(1). The ring position so obtained also supported the NOEs that were observed between the indole ring and the N-terminal protecting group.

Table 4. **Backbone torsion angles (in °) in nuclear magnetic resonance (NMR)-derived structures obtained for peptide 2[a]**

Number	Residue	Angle	Mol 1	Mol 25	Mol 50	Mean
1	Leu	ψ	−30.5	−25.5	−30.5	−31.3
2	Trp	ω	−180.0	−180.0	−180.0	−180.0
2	Trp	ϕ	−61.4	−59.0	−62.9	−61.7
2	Trp	ψ	−34.9	−25.1	−34.9	−32.4
3	Val	ω	−180.0	−179.9	−179.9	180.0
3	Val	ϕ	−62.9	−60.0	−62.3	−62.1
3	Val	ψ	−34.5	−31.5	−33.3	−32.8
4	Aib	ω	175.8	175.8	175.9	175.8
4	Aib	ϕ	−56.1	−57.8	−58.0	−60.5
4	Aib	ψ	−34.9	−30.5	−34.0	−30.8
5	Ala	ω	−179.9	179.9	−180.0	−180.0
5	Ala	ϕ	−65.3	−65.4	−65.7	−65.4
5	Ala	ψ	−30.9	−25.0	−24.8	−27.8
6	Aib	ω	175.8	175.8	175.9	175.8
6	Aib	ϕ	−56.3	−55.8	−65.2	−56.6
6	Aib	ψ	−25.0	−24.9	−31.4	−26.3
7	Leu	ω	180.0	180.0	−180.0	180.0
7	Leu	ϕ	−55.7	−55.5	−55.4	−56.1
7	Leu	ψ	−25.0	−25.0	−24.8	−24.9
8	Trp	ω	−180.0	180.0	180.0	−180.0
8	Trp	ϕ	−55.3	−55.4	−54.9	−55.2
8	Trp	ψ	−35.0	−35.1	−35.0	−33.5
9	Val	ω	180.0	−180.0	−180.0	180.0
9	Val	ϕ	−65.1	−63.6	−64.2	−64.5

a. Mol 1, Mol 25 and Mol 50 correspond to structures 1, 25 and 50 of the 50 calculated NMR structures.

Similarly, the indole ring of Trp(8) gave NOEs to the C-terminal protecting group. In this case, the ring positions in the calculated structure were obtained from NOEs observed between the side chain of Trp(8) and Val(9). The RMSD for the backbone atoms for a family of 50 structures is 0.21 ± 0.08 Å and the mean global heavy atom RMSD is 0.82 ± 0.22 Å. Superposition of the calculated 50 structures was carried out using MOLMOL, and is shown along with the mean structure, in Fig. 9. Backbone torsion angles calculated for three of the 50 structures are listed in Table 4.

The backbone (NH and $C^{\alpha}H$ protons) chemical shifts for peptides **1** and **2** compare well with those obtained for the tripeptide Boc-Leu-Trp-Val-OMe and Boc-Ala-Aib-Leu-Trp-Val-OMe (35). In the tripeptide, the Leu and Trp residues adopt helical ϕ–ψ values, with the dipeptide segment forming a type I β-turn in crystals. In the pentapeptide, a short stretch of 3_{10}-helix is formed over the segment -Ala-Aib-Leu-Trp- in the solid state (35). The chemical shifts of the $C^{\alpha}H$ resonances of the Leu-Trp-Val segment of both the tripeptides and pentapeptides correlated well with the C-terminal segment of the longer peptides. Backbone chemical shifts were essentially invariant between residues of peptides **1** and **2**, indicating that the two peptides did adopt identical conformations. Crystals suitable for X-ray diffraction were obtained only for peptide **1**. Hence, comparison of the 1D chemical shift dispersion of both the peptides (**1** and **2**) further aids in complete assessment of the solution structure of peptide **2**.

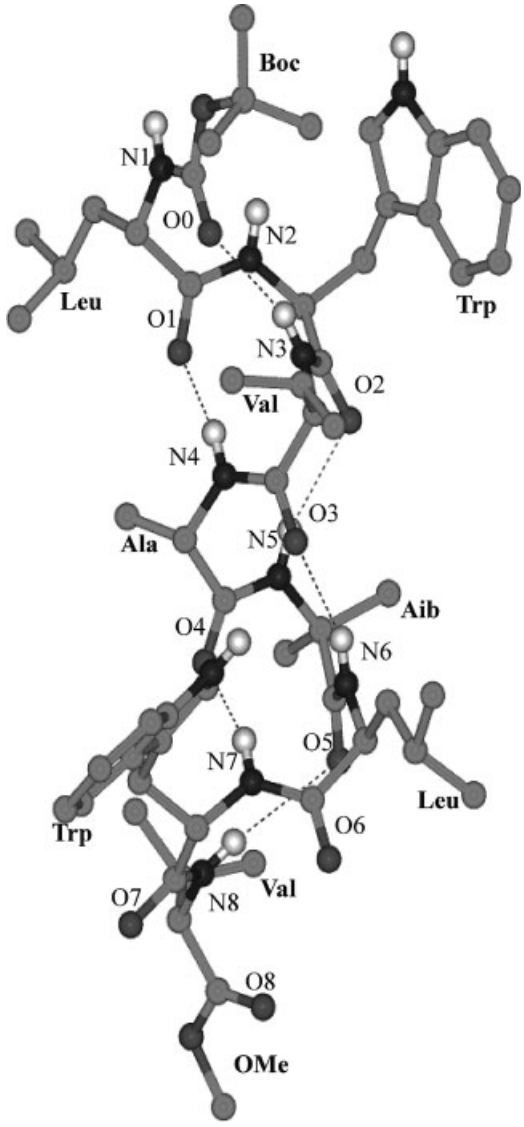

Figure 10. Molecular conformation of Boc-Leu-Trp-Val-Ala-Aib-Leu-Trp-Val-OMe, **1**, in crystals. The intramolecular hydrogen bonds are shown by dotted lines.

Conformation of peptide 1 in crystals

The molecular conformation of peptide **1** in the crystal state, determined by X-ray diffraction, is illustrated in

Table 5. **Hydrogen bond parameters for peptide 1 in the crystal structure of Boc-Leu-Trp-Val-Ala-Aib-Leu-Trp-Val-OMe**

Type	Donor (D)	Acceptor (A)	D…A (Å)	H…A (Å)	C=O…H (°)	C=O…D (°)	OH…D (°)
Intramolecular							
4 → 1[a]	N(3)	O(0)	3.084	2.253	127.8	131.0	162.6
4 → 1[a]	N(4)	O(1)	2.959	2.141	123.2	128.9	158.8
4 → 1[a]	N(5)	O(2)	3.169	2.335	117.8	122.1	163.5
4 → 1[a]	N(6)	O(3)	3.142	2.330	126.7	130.0	157.6
4 → 1[a]	N(7)	O(4)	2.927	2.102	119.6	125.2	160.5
4 → 1	N(8)	O(5)	3.513	2.658	111.5	113.4	172.4
Intermolecular							
	N(1)[a]	O(7)[b]	2.972	2.122	117.3	119.6	169.5
	N(2ε1)[a]	O(6)[b]	2.860	2.193	145.1	150.9	134.3
	N(2)	O(8)[b]	3.390	2.830	125.7	119.8	124.3

a. These are acceptable hydrogen bonds.
b. Symmetry related by the relation ($x + 1$, y, $z - 1$).

Table 6. **Torsion angles (in °) in the crystal state conformations of peptides 1, 3, and 4**

	Peptide **1**			Peptide **3**			Peptide **4**		
Residue	φ	ψ	ω	φ	ψ	ω	φ	ψ	ω
Backbone conformations									
Leu(1)	−60.7	−28.1	180.0				−76.8	−11.6	−177.1
Trp(2)	−62.2	−21.1	176.0				−91.0	−8.8	−170.7
Val(3)	−64.5	−20.5	179.2				−62.7	150.4	175.0
Ala(4)	−59.5	−23.8	−178.9	−58.7	−28.1	−178.2			
Aib(5)	−50.7	−39.4	−173.7	−50.2	−37.1	−173.9			
Leu(6)	−66.8	−20.5	−172.2	−77.2	−14.2	−162.9			
Trp(7)	−94.0	−6.0	−176.6	−123.2	4.8	177.0			
Val(8)	−92.3	170.8	179.8	−92.5	−19.2	−175.5			

	Peptide **1**		Peptide **3**		Peptide **4**	
	χ^1	χ^2	χ^1	χ^2	χ^1	χ^2
Side chains conformations						
Leu(1)	179.8	61.7	–	–	−57.3	−57.2
		−175.8				177.1
Trp(2)	53.4	83.1	–	–	53.4	80.6
		−95.6				−99.1
Val(3)	78.0		–	–	67.8	
	−159.0				−164.1	
Leu(6)	−175.8	57.6	−60.6	−39.5		
		−180.0		−165.4		
Trp(7)	−63.4	66.3	−64.0	−67.4		
		−111.9		110.9		
Val(8)	−62.6		−62.6			
	67.8		65.1			

Peptide **1**, Boc-Leu-Trp-Val-Ala-Aib-Leu-Trp-Val-OMe; peptide **2**, Boc-Ala-Aib-Leu-Trp-Val-OMe; peptide **3**, Boc-Leu-Trp-Val-OMe.

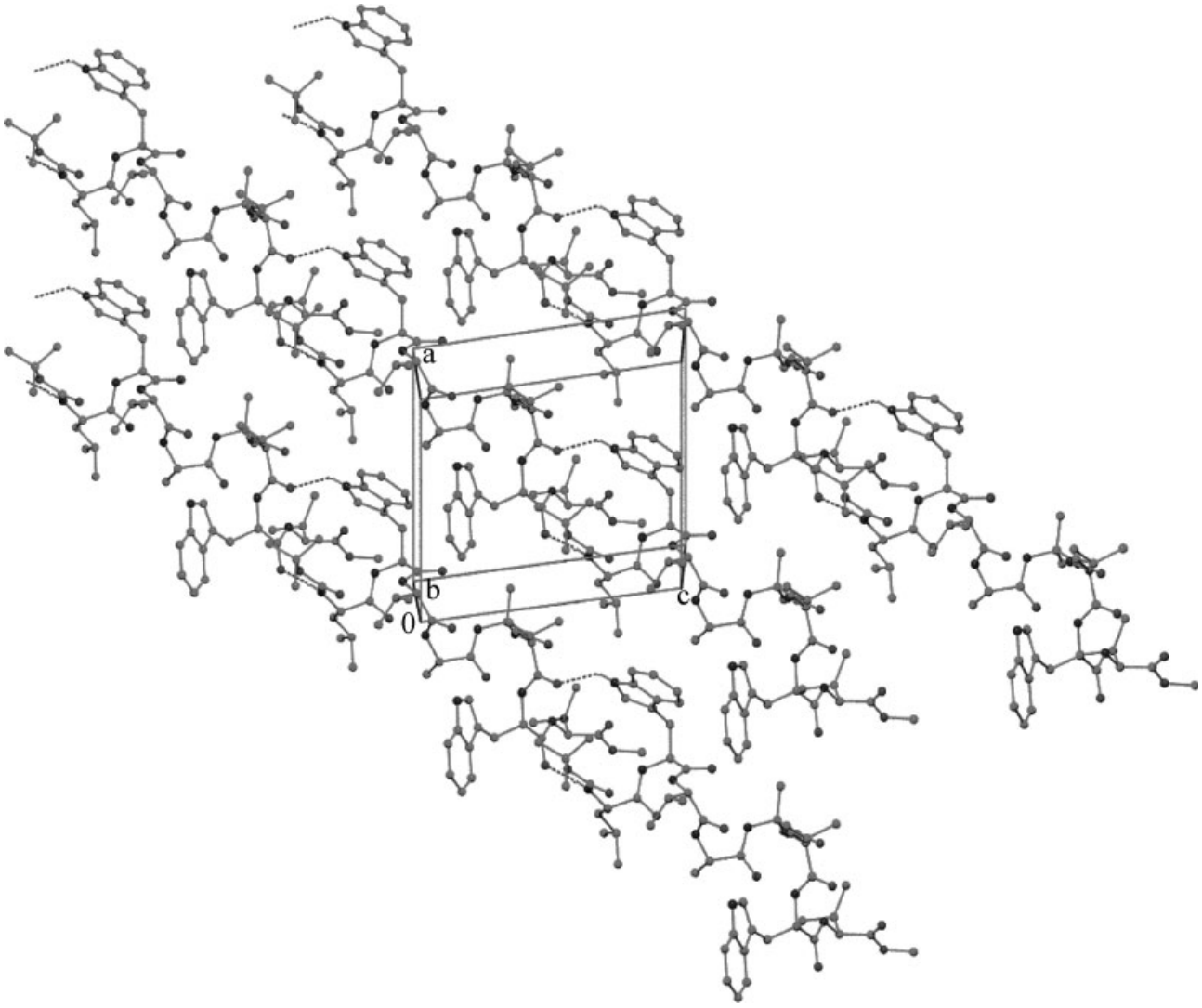

Figure 11. Packing diagram for peptide **1** viewed down the *b*-axis. Helical columns run along the *a*/*c* diagonal of the unit cell.

Fig. 10. Potential intramolecular and intermolecular hydrogen bond parameters are listed in Table 5, while the relevant backbone and side chain torsion angles are given in Table 6. Inspection of the hydrogen bond parameters in Table 5 reveals that the molecule is stabilized by five strong intramolecular $4 \rightarrow 1$ hydrogen bonds, corresponding to a 3_{10}-helical fold over the sequence of residues 1–7. The average values of the torsion angles ϕ and ψ for residues 1–6°, −60.7° and −25.6°, are very close to those expected for an ideal right-handed 3_{10}-helix ($\phi = -60°$, $\psi = -30°$). The values obtained for Trp(7) ($\phi = -94°$, $\psi = -6.0°$) are significantly distorted from the ideal 3_{10}-helical values. The C-terminal residue Val(8) adopts an extended conformation. Table 6 also lists the backbone torsion angles determined in an earlier study for the pentapeptide (Boc-Ala-Aib-Leu-Trp-Val-OMe), **3** and the tripeptide (Boc-Leu-Trp-Val-OMe), **4** (35). The sequences of **3** and **4** correspond to the C-terminus and N-terminus of peptide **1**, respectively.

The backbone conformation for residues 1–8 determined in the crystal compares well with that determined in solution by NMR. A notable feature of peptide **1** is that the introduction of a single centrally positioned Aib residue has successfully resulted in nucleating a helical conformation over a 7-residue stretch of the peptide.

Crystal packing

Peptide **1** crystallizes in the triclinic space group P1, resulting in a parallel assembly of peptide helices in the crystal. A view perpendicular to the helix axis is illustrated in Fig. 11. Helical columns are formed by head-to-tail

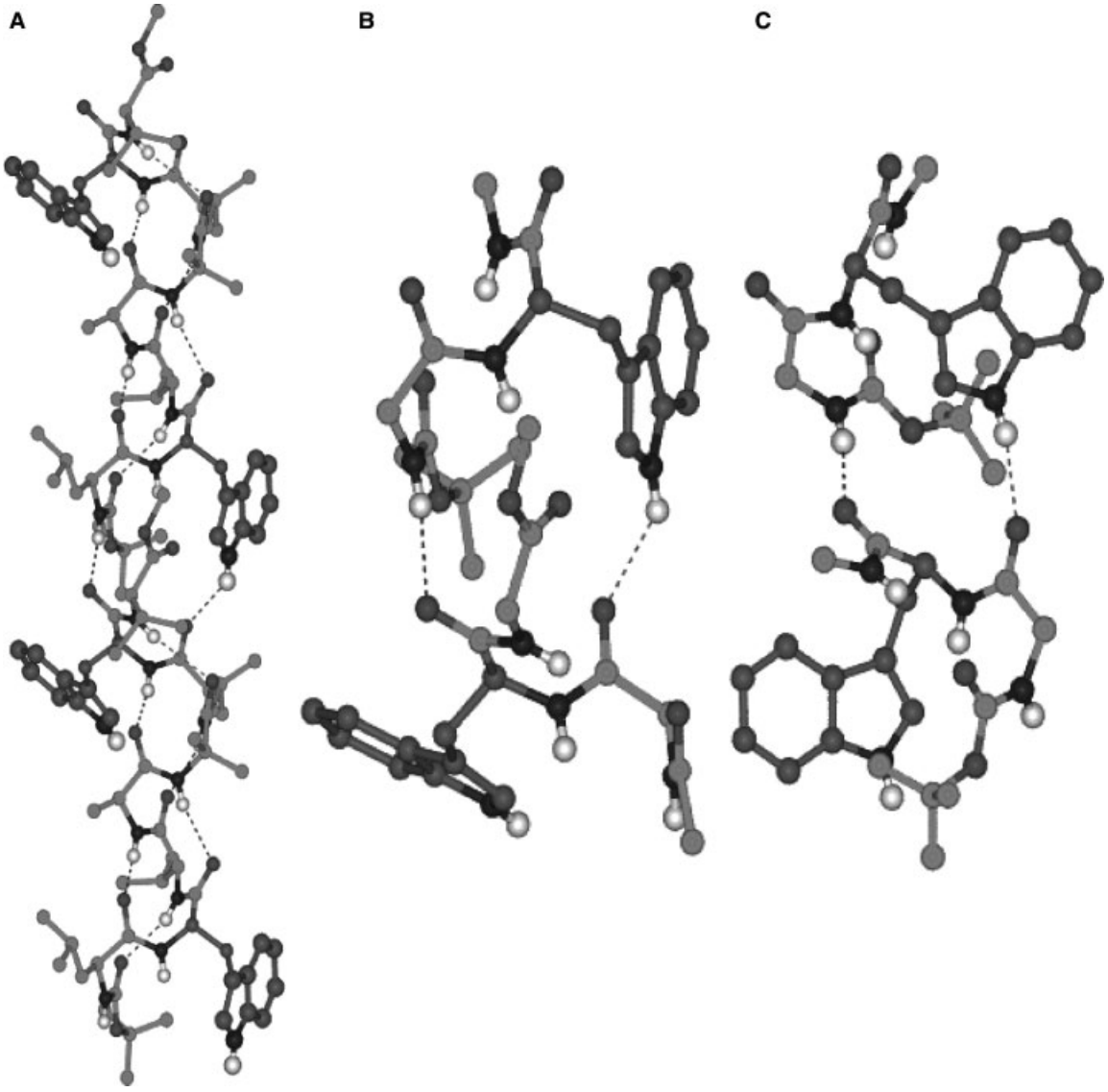

Figure 12. (A) View of the helical column of peptide **1** stabilized by intermolecular hydrogen bonds [Trp(2)Nε1H…OCLeu(6) and Leu(1)-NH…OCTrp(7)]. (B) An expanded view of the stabilizing intermolecular hydrogen bonding interactions driving the packing of molecules in the crystals of peptide **1**, compared with that observed in peptide **4** (C).

assembly of helical rods, stabilized by two strong intermolecular hydrogen bonds, Leu(1)NH…OCTrp(7) [N…O = 2.971 Å] and indole of Trp(2) Nε1H…OCLeu(6) [N…O = 2.861 Å] between the symmetry-related molecules. A third potential hydrogen bond interaction between Trp(2)-NH…OCVal(8) (N…O = 3.390 Å; H…O = 2.830 Å; $\angle$NH…O = 124.3°) is less than optimal (Fig. 12A). Figure 12B shows an expanded view of the intermolecular hydrogen bonds, which stabilize the helical column arrangement. Interestingly, an almost identical hydrogen bond pattern, which includes a Trp Nε1H–backbone carbonyl interaction is also observed in the crystal structure of the tripeptide Boc-Leu-Trp-Val-OMe (**4**) (Fig. 12C). Indeed, in an earlier study, the formation of a helical 'supermolecule' in crystals has been noted (35). The conservation of this packing motif in the octapeptide suggests a special stability associated with this mode of assembly.

Indole NH groups of Trp residues in proteins and peptides are most often involved in hydrogen bond interactions. A survey of the structures available in the Cambridge Crystallographic Database (34) reveals that the overwhelming majority of examples have the indole NH hydrogen bonded to a suitable acceptor (Table 7). Interestingly, peptide **1** provides an example of a nonhydrogen bonded indole NH, with the Nε1H of the Trp(7) residue being uninvolved in any interaction. Figure 13 shows a view of the environment of Trp(7) indole ring. Trp(2) and Trp(7), of a symmetry-related molecule, are closely packed in an orthogonal

Table 7. **Indole NH interaction in Trp peptide crystal structures**

Sequences	Secondary structures	Role of indole Nε1H	Database identification	References
Boc-Leu-Trp-Val-OMe	Type I β-turn	Trp(2)Nε1H…OCLeu(1)	220248	(35)
Ac-Leu-Trp-Val-OMe				
$P2_1$ (polymorph)	β-sheet	Trp(2)Nε1H…OCVal(3)	247188	(35)
$P2_12_12_1$ (polymorph)	β-sheet	Trp(2)Nε1H…OCVal(3)	247187	(35)
Boc-Ala-Aib-Leu-Trp-Val-OMe	3_{10}-helix	Trp(4)Nε1H…OW	247186	(35)
Boc-Leu-Trp-Val-Ala-Aib-Leu-Trp-Val-OMe	3_{10}-helix	Trp(2)Nε1H…OCLeu(1)		Present study
		Trp(7)Nε1H not hydrogen bonded		
Boc-Gly-Trp-Ala-O-*t*-Bu	Type I β-turn	Trp(2)Nε1H…OCGly(1)	TUPGOA	(49)
Z-Aib-Trp-Aib-OMe				
Mol A	Type III/I β-turn	Trp(2)Nε1H…OCAib(1) (Mol B)	ROHVEP	(50)
Mol B	Type I β-turn	Trp(2)Nε1H…OCAib(1) (Mol A)		
Z-Aib-Aib-Trp-Aib-OMe	3_{10}-helix	Trp(3)Nε1H…OCH_3OH	ROHVIT	(50)
Z-Aib-Aib-Aib-Trp-Aib-O-*t*-Bu	3_{10}-helix	Trp(4)Nε1H…$NCCH_3$	ROHVOZ	(50)
Boc-Aib-Aib-Aib-Trp-Aib-OMe	3_{10}-helix	Trp(4)Nε1H…OCTrp(4)	ROHVUF	(50)
Leu-Trp-Leu hydrochloride dihydrate	β-sheet	Trp(2)Nε1H…Cl	FUDFUF	(51)
Boc-Gly-Val-Trp-OMe	β-sheet	Trp(3)Nε1H…OCBoc(0)	–[a]	(52)
		(intramolecular hydrogen bond)		
Gly-Trp dihydrate	–	Trp(2)Nε1H not hydrogen bonded	GLTRDH01	(53)
Ala-Trp monohydrate	–	Trp(2)Nε1H not hydrogen bonded	FUJZUF	(53)
Trp-Gly monohydrate	–	Trp(1)Nε1H…OC(COO^-)	FULGEY	(53)
Trp-Gly-Gly dihydrate	–	Trp(1)Nε1H…OCGly(3)	FIZWOA01	(54)
Trp-Met-Asp-phenylalanylamide				
Mol A		Trp(1)Nε1H…$OHCH_3$	GASTRN10	(55)
Mol B	–	Trp(1)Nε1H… $OHCH_3$		
7-methylguanosine-5′-phosphate-Trp-Glu complex	–	Trp(1)Nε1H…OW	SEKXIP10	(56)
Boc-Aib-Trp-$(Leu\text{-}Aib\text{-}Ala)_2$-Phe-Aib-OMe	$3_{10}/\alpha$-helix	Trp(2)Nε1H…OCAib(10)	HICKEJ	(57)
Boc-Trp-$(Leu\text{-}Aib\text{-}Ala)_2$-Phe-Aib-OMe	3_{10}-helix	Trp(1)Nε1H…OCPhe(8)	–[a]	(57)
Boc-Trp-Ile-Ala-Aib-Ile-Val-Aib-Leu-Aib-Pro-OMe				
$P2_1$ (polymorph)	$3_{10}/\alpha$-helix	Trp(1)Nε1H…OCAib(9)	–[a]	(58)
		Trp(1)Nε1H…OCPro(10)		
P1 (polymorph)	$3_{10}/\alpha$-helix	Trp(1)Nε1H…OCLeu(8)	–[a]	(59)
		Trp(1)Nε1H…OCAib(9)		
Ac-Trp-Ile-Ala-Aib-Ile-Val-Aib-Leu-Aib-Pro-OMe	$3_{10}/\alpha$-helix	Trp(1)Nε1H…OCAib(7)	–[a]	(59)

a. These coordinates are not available in the Cambridge Crystallographic Database and were taken directly from the reported papers.

arrangement of the indole rings. The C2ζ3H of Trp(2) is directly positioned over the plane of the 6-membered ring of Trp(7), suggestive of a strong CH…π interaction (18). This Trp–Trp interaction may be an important stabilizing factor in bringing adjacent helical columns together in the crystal. Thus, assembly of peptide **1** into crystals may be facilitated by two important interactions involving the bulky Trp residues: first, the Trp(2) Nε1H mediates columnar assembly of helices and secondly, aromatic interactions between Trp(2) and Trp(7) of neighboring molecules brings the columns together in the crystal.

The observed packing arrangement in crystals of **1** may be compared with that observed in crystals of the tripeptide (Boc-Leu-Trp-Val-OMe) **4**. Peptide **4** crystallizes in the tetragonal space group $P4_3$. The major stabilizing interactions are the intermolecular hydrogen bonds formed between Leu(1) NH…OC Trp(2) and Trp(2) Nε1H with a backbone C=O group of a symmetry-related molecule,

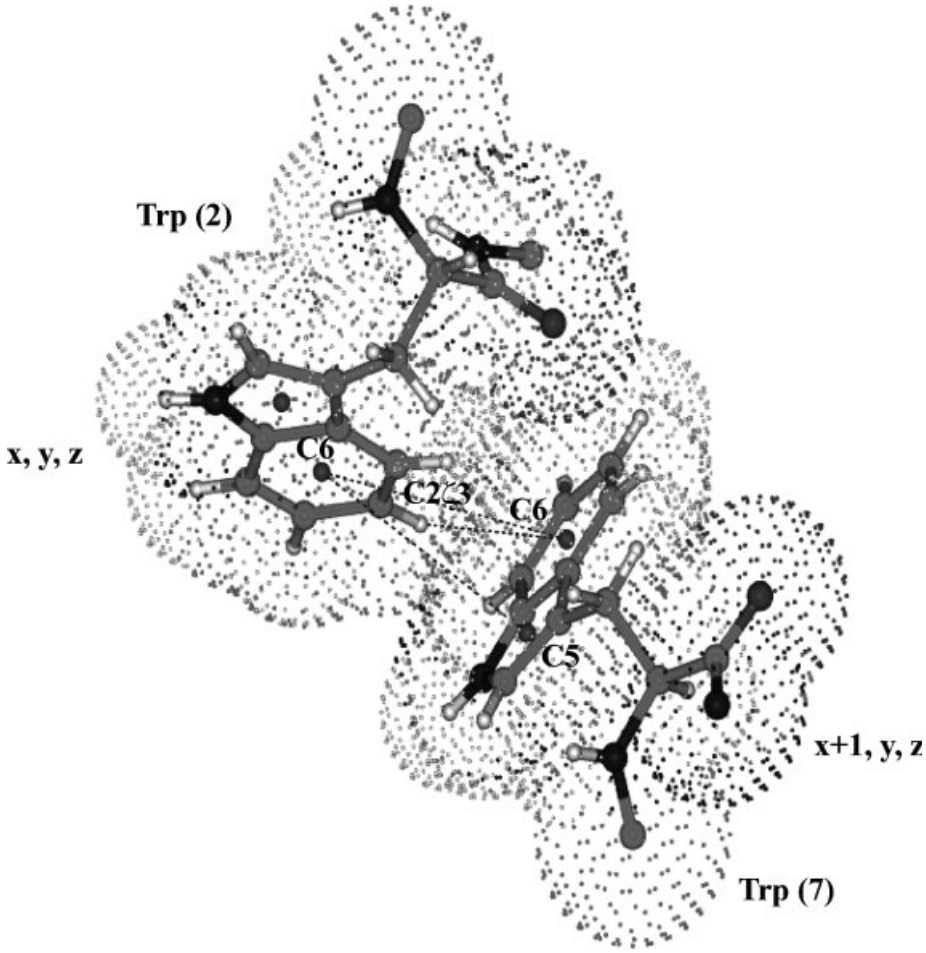

Figure 13. Close packing of the two Trp rings observed in the crystals of peptide **1** (the van der Waals surfaces are shown). The parameters defining aromatic interactions are: R_{6cen} = C6…C6 = 5.72 Å; R_{5cen} = C5…C5 = 6.77 Å; $R_{6,5cen}$ = C6…C5 = 4.87 Å; interplanar angle (γ) = 70.5°; C2ζ3…C6 = 4.41 Å; H2ζ3…C6 = 3.51 Å; $\angle$CH…π = 163.8°.

which results in a quasihelical arrangement of the assembly of the tripeptide. Here again, Trp–Trp interactions mediate close packing of molecules in the crystal.

Monitoring peptide association by NMR

The crystal structure suggests that two dominant interactions involving the Trp side chains are important in determining the observed mode of packing. These are: (i) intermolecular hydrogen bonding involving the Trp(2) Nε1H group, and (ii) an edge-to-face interaction of Trp(2) and Trp(7) on neighboring molecules. The former facilitates helical column formation while the latter permits lateral association of neighboring columns. It was therefore of interest to probe whether peptide aggregates, which might serve as nuclei for crystallization, are indeed formed in solution. Figure 14 illustrates the indole ring proton chemical shifts in peptides **1** and **2**. Data for the fragments Boc-Ala-Aib-Leu-Trp-Val-OMe (peptide **3**) and Boc-Leu-Trp-Val-OMe (peptide **4**) are also shown. In both peptides **1** and **2**, the ring protons of resonances Trp(2) and Trp(7/8) are clearly distinguishable. A notable feature is the downfield position of the Trp(2) Nε1H proton in both peptides **1** and **2**, when compared with the indole NH proton of Trp(7) in **1** and Trp(8) in **2** and the Trp residues in the pentapeptide and tripeptide fragments. Interestingly, it is the Trp(2) Nε1H proton which forms an intermolecular hydrogen bond in crystals resulting in helical column formation in peptide **1**. Figure 14 inset shows the concentration dependence of the Trp(2) and Trp(7) indole NH resonances as a function of peptide concentration over the range 0.2–10 mM. The Trp(2) NH shows a marked concentration dependence, while the Trp(7) NH chemical shift is largely insensitive, clearly supporting side chain–backbone-mediated helical column formation in solution. No NOEs could be detected between the ring protons of Trp(2) and Trp(7/8) in peptides **1** and **2**. The chemical shifts of the Cζ3H proton of Trp(2) appeared

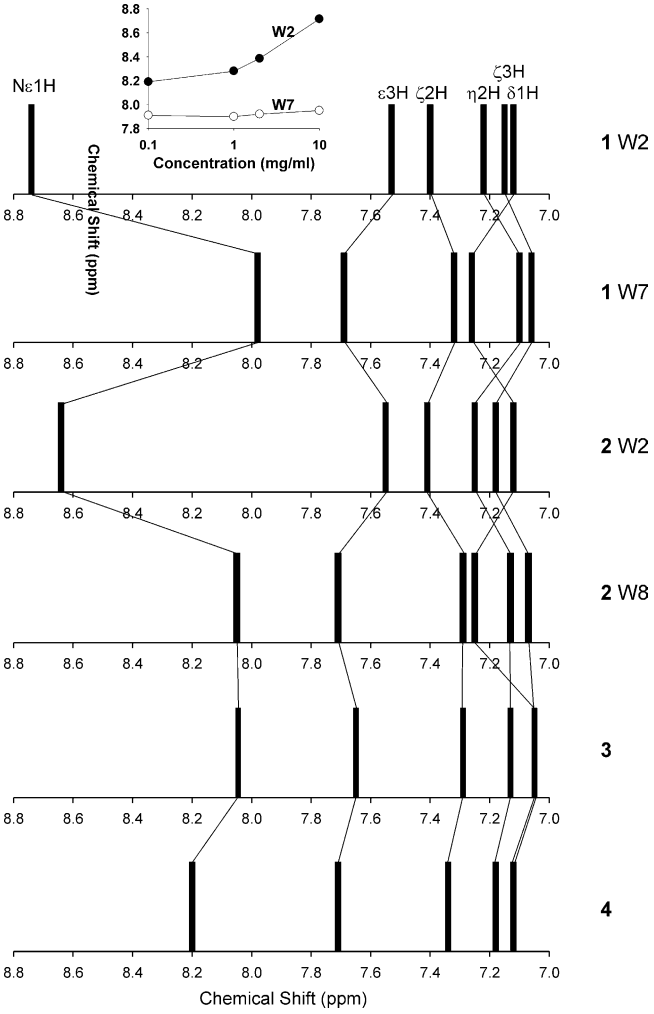

Figure 14. Stick plots of the ring proton resonances of peptides **1** and **2** compared with the Trp(4) indole resonances of the pentapeptide Boc-Ala-Aib-Leu-Trp-Val-OMe (**3**) and Trp(2) of the tripeptide Boc-Leu-Trp-Val-OMe (**4**). All spectra were recorded in $CDCl_3$ at 300 K. Inset: concentration dependence of the indole Nε1H resonances of Trp(2) and Trp(7) in peptide **1** (*X*-axis in logarithmic scale).

in the range normally expected for indole ring suggesting that at the concentrations studied, lateral association of helical columns was insignificant. The NMR studies establish that peptide association in chloroform does not involve any dramatic change of the helical conformation; rather, preformed helices self-associated with the indole NH of residue 2, providing a stabilizing intermolecular hydrogen bond to an acceptor C=O group of another molecule.

Conclusion

The studies of peptide helices containing two Trp residues provide evidence for the role of the indole side chain in facilitating intermolecular interactions. Indole rings act as both hydrogen bond donors and weak hydrogen bond acceptors in potential C-H…π interactions. The positioning of indole rings of Trp residues at specific sites on helical scaffolds may provide an opportunity to engineer peptide association by designing intermolecular interactions.

Acknowledgements: RM is supported by the award of a Senior Research Fellowship (SRF) from the Council of Scientific and Industrial Research (CSIR), India. The CCD diffractometer facility is supported under the IRHPA program of the Department of Science and Technology, Government of India. This work is supported by grants from the CSIR, India and a program in the area of Molecular Diversity and Design funded by the Department of Biotechnology, India.

References

1. Burley, S.K. & Petsko, G.A. (1985) Aromatic-aromatic interaction: a mechanism of protein structure stabilization. *Science* **229**, 23–28.
2. Hunter, C.A. & Sanders, J.K.M. (1990) The nature of π-π interactions. *J. Am. Chem. Soc.* **112**, 5525–5534.
3. Sun, S. & Bernstein, E.R. (1996) Aromatic van der Waals clusters: structure and non-rigidity. *J. Phys. Chem.* **100**, 13348–13366.
4. Hunter, C.A., Lawson, K.R., Perkins, J. & Urch, C.J. (2001) Aromatic interactions. *J. Chem. Soc. Perkin Trans.* **2**, 651–669.
5. Ishida, T., Iyo, H., Ueda, H., Doi, M., Inoue, M., Nishimura, S. & Kitamaura, K. (1991) Interaction of indole derivatives with biologically important aromatic compounds. Importance of simultaneous co-operation of hydrogen-bond pairing and stacking interactions for recognition of guanine base by a peptide: X-ray crystal analysis of 7-methylguanosine-5′-phosphate-tryptophanylglutamic acid complex. *J. Chem. Soc. Perkin Trans.* **1**, 1847–1853.
6. Chakrabarti, P. & Samanta, U. (1995) C-H/π interaction in the packing of the adenine ring in protein structures. *J. Mol. Biol.* **251**, 9–14.
7. Samanta, U. & Chakrabarti, P. (2001) Assessing the role of tryptophan residues in the binding site. *Protein Eng.* **14**, 7–15.
8. Macias, M., Wiesner, S. & Sudol, M. (2002) WW and SH_3 domains, two different scaffolds to recognize proline-rich ligands. *FEBS Lett.* **513**, 30–37.
9. Gazit, E. (2002) A possible role for π-stacking in the self-assembly of amyloid fibrils. *FASEB J.* **16**, 77–83.
10. Tracz, S.M., Abedini, A., Driscoll, M. & Raleigh, D.P. (2004) Role of aromatic interactions in amyloid formation by peptides derived from human amylin. *Biochemistry* **43**, 15901–15908.

11. Burley, S.K. & Petsko, G.A. (1988) Weakly polar interactions in proteins. *Adv. Protein Chem.* **39**, 125–189.
12. Gervasio, F., Chelli, R., Procaccino, P. & Schettino, V. (2002) The nature of intermolecular interactions between aromatic amino acid residues. *Proteins: Struct. Funct. Genet.* **48**, 117–125.
13. Samanta, U., Pal, D. & Chakrabarti, P. (1999) Packing of aromatic rings against tryptophan residues in proteins. *Acta Crystallogr.* **D55**, 1421–1427.
14. Samanta, U., Pal, D. & Chakrabarti, P. (2000) Environment of tryptophan side chains in proteins. *Proteins: Struct. Funct. Genet.* **38**, 288–300.
15. Burley, S.K. & Petsko, G.A. (1986) Amino-aromatic interactions in proteins. *FEBS Lett.* **203**, 139–143.
16. Levitt, M. & Perutz, M.F. (1988) Aromatic rings as hydrogen bond acceptors. *J. Mol. Biol.* **201**, 751–754.
17. Pejov, L. (2001) A gradient-corrected density functional study of indole self-association through N-H…π hydrogen bonding. *Chem. Phys. Lett.* **339**, 269–278.
18. Brandl, M., Weiss, M.S., Jabs, A., Suhnel, J. & Hilgenfeld, R. (2001) C-H...π-interactions in proteins. *J. Mol. Biol.* **307**, 357–377.
19. Nakamura, H. (1996) Roles of electrostatic interaction in proteins. *Q. Rev. Biophys.* **29**, 1–90.
20. Chelli, R., Gervasio, F.L., Procacci, P. & Schettino, V. (2002) Stacking and T-shape competition in aromatic-aromatic amino acid interactions. *J. Am. Chem. Soc.* **124**, 6133–6143.
21. Neidigh, J.W., Fesinmeyer, R.M. & Anderson, N.H. (2002) Designing a 20-residue protein. *Nat. Struct. Biol.* **9**, 425–430.
22. Klein-Seetharaman, J., Oikawa, M., Grimshaw, S.B., Wirmer, J., Duchardt, E., Ueda, T., Imoto, T., Smith, L.J., Dobson, C.M. & Schwalbe, H. (2002) Long-range interactions within a nonnative protein. *Science* **295**, 1719–1722.
23. Cochran, A.G., Skelton, N.J. & Starovasnik, M.A. (2001) Tryptophan zippers: stable, monomeric β-hairpins. *Proc. Natl Acad. Sci U S A* **98**, 5578–5583.
24. Yau, W.-M., Wimley, W.C., Gawrisch, K. & White, S.H. (1998) The preference of tryptophan for membrane interfaces. *Biochemistry* **37**, 14713–14718.
25. Eilers, M., Shekar, S.C., Shieh, T., Smith, S.O. & Flemming, P.J. (2000) Internal packing of helical membrane proteins. *Proc. Natl Acad. Sci U S A* **97**, 5796–5801.
26. Schiffer, M., Chang, C.-H. & Stevens, F. (1992) The functions of tryptophan residues in membrane proteins. *Protein Eng.* **5**, 213–214.
27. Hu, W., Lee, K.-C. & Cross, T.A. (1993) Tryptophans in membrane proteins: indole ring orientations and functional implications in the gramicidin channel. *Biochemistry* **32**, 7035–7047.
28. Doyle, D. & Wallace, B. (1997) Crystal structures of the gramicidin/potassium thiocynate complex. *J. Mol. Biol.* **266**, 963–977.
29. Bingham, N.C., Smith, N.E.C., Cross, T.A. & Busath, D.D. (2003) Molecular dynamic simulations of Trp side chain conformational flexibility in the gramicidin A channel. *Biopolymers (Pept. Sci.)* **71**, 593–600.
30. Langs, D.A. (1989) Structure of the ion channel peptide antibiotic gramicidin A. *Biopolymers* **28**, 259–266.
31. Callis, P.R. (1997) ^1L_a and ^1L_b transitions of tryptophan: applications to theory and experimental observations to fluorescence of proteins. *Methods Enzymol.* **278**, 113–150.
32. Chakrabarti, P. & Pal, D. (1998) Main-chain conformational features at different conformations of the side-chains in proteins. *Protein Eng.* **11**, 631–647.
33. Thomas, A., Meurisse, R., Charloteaux, B. & Brasseur, R. (2002) Aromatic side-chain interactions in proteins: I. Main structural features. *Proteins* **48**, 628–634.
34. Allen, F.H. (2002) The Cambridge Structural Database: a quarter of a million crystal structures and rising. *Acta Crystallogr.* **B58**, 380–388.
35. Sengupta, A., Mahalakshmi, R., Shamala, N. & Balaram, P. (2005) Aromatic interactions in tryptophan-containing peptides: crystal structures of model tryptophan peptides and phenylalanine analogs. *J. Pept. Res.* **65**, 113–129.
36. Prasad, B.V.V. & Balaram, P. (1984) The stereochemistry of peptides containing α-aminoisobutyric acid. *CRC Crit. Rev. Biochem.* **16**, 307–348.
37. Balaram, H., Sukumar, M. & Balaram, P. (1986) Stereochemistry of α-aminoisobutyric acid peptides in solution. Conformations of decapeptides with a central triplet of contiguous L-amino acids. *Biopolymers* **25**, 2209–2223.
38. Braunschweiler, L.E. & Ernst, R.R. (1983) Coherence transfer by isotropic mixing: application to proton correlation spectroscopy. *J. Magn. Reson.* **53**, 521–528.
39. Bothner-By, A.A., Stephens, R.L., Lee, J., Warren, C.D. & Jeanloz, R.W. (1984) Structure determination of a tetrasaccharide: transient nuclear Overhauser effects in the rotating frame. *J. Am. Chem. Soc.* **106**, 811–812.
40. Bax, A. & Davis, D.G. (1985) Practical aspects of two-dimensional transverse NOE spectroscopy. *J. Magn. Reson.* **63**, 207–213.
41. Pitner, T.P. & Urry, D.W. (1972) Proton magnetic resonance studies in trifluoroethanol. Solvent mixtures as a means of delineating peptide protons. *J. Am. Chem. Soc.* **94**, 1399–1400.
42. Iqbal, M. & Balaram, P. (1981) The 3_{10} helical conformation of the amino terminal decapeptide of suzukacillin. 270 MHz ^{1}H NMR evidence for eight intramolecular hydrogen bonds. *J. Am. Chem. Soc.* **103**, 5548–5552.
43. Raj, P.A. & Balaram, P. (1985) Conformational effects on peptide aggregation in organic solvents. Spectroscopic studies of two chemotactic tripeptide analogs. *Biopolymers* **24**, 1131–1146.
44. Guntert, P., Mumenthaler, C. & Wuthrich, K. (1997) Torsion angle dynamics for NMR structure calculation with the new program DYANA. *J. Mol. Biol.* **273**, 283–298.
45. Koradi, R., Billeter, M. & Wuthrich, K. (1996) MOLMOL: a program for display and analysis of macromolecular structures. *J. Mol. Graph.* **14**, 51–55.
46. Schneider, T.R. & Sheldrick, G.M. (2002) Substructure solution with SHELXD. *Acta Crystallogr.* **D58**, 1772–1779.
47. Sheldrick, G.M. (1997) *SHELXL*-97: Program for the Refinement of Crystal Structures. University of Gottingen, Gottingen, Germany.
48. Aravinda, S., Datta, S., Shamala, N. & Balaram, P. (2004) Hydrogen-bond lengths in polypeptide helices: no evidence for short hydrogen bonds. *Angew. Chem. Int. Ed. Engl.* **43**, 6728–6731.
49. Anthoni, U., Christophersen, C., Flensburg, C., Jakobsen, M.H., Jensen, J. & Nielsen, P.H. (1996) Tryptophan-derived peptides: 1. Crystal structure and solution conformation of Boc-Gly-Trp-Ala-OtBu. *Struct. Chem.* **7**, 103–110.
50. George, C., Flippen-Anderson, J.L., Bianco, A., Crisma, M., Formaggio, F. & Toniolo, C. (1996) Crystallographic characterization of tryptophan-containing peptide 3_{10}-helices. *Pept. Res.* **9**, 315–321.

51. Wu, S., Declercq, J.P., Tinant, B. & Meerssche, M.V. (1987) Crystal structure and conformation of short linear peptides: Part VIII. L-leucyl-L-tryptophanyl-L-leucine hydrochloride dihydrate. *Bull. Soc. Chim. Belg.* **96**, 581–586.
52. Banumathi, S., Velmurugan, D., Subramanian, E., Katti, S.B. & Haq, W. (1998) Methyl N-(tert-butoxycarbonyl)-glycyl-L-valyl-L-tryptophanate. *Acta Crystallogr.* **C54**, 1681–1683.
53. Emge, T.J., Agrawal, A., Dalessio, J.P., Dukovic, G., Inghrim, J.A., Janjua, K., Macaluso, M., Robertson, L.L., Stiglic, T.J., Volovik, Y. & Georgiadis, M.M. (2000) Alaninyltryptophan hydrate, glycyltryptophan dihydrate and tryptophylglycine hydrate. *Acta Crystallogr.* **C56**, e469–e471.
54. Subramanian, E. & Sahayamary, J.J. (1989) Structure and conformation of linear peptides. *Int. J. Pept. Protein Res.* **34**, 134–138.
55. Cruse, W.B.T., Egert, E., Viswamitra, M.A. & Kennard, O. (1982) The structure of the hydrochloride salt of Trp-Met-Asp-Phe-NH_2.CH_3OH.0.5$C_2H_5OC_2H_5$, the C-terminal tetrapeptide amide of gastrin. *Acta Crystallogr.* **B38**, 1758–1764.
56. Ishida, T., Iyo, H., Ueda, H., Doi, M., Inoue, M., Nishimura, S. & Kitamura, K. (1991) Interaction of indole derivatives with biologically important aromatic compounds. Importance of simultaneous co-operation of hydrogen-bond pairing and stacking interactions for recognition of guanine base by a peptide: X-ray crystal analysis of 7-methylguanosine-5′-phosphate-tryptophanylglutamic acid complex. *J. Chem. Soc. Perkin Trans.* **1**, 1847–1853.
57. Karle, I.L., Flippen-Anderson, J.L., Gurunath, R. & Balaram, P. (1994) Facile transition between 3_{10} and α-helix: structures of 8-, 9-, and 10-residue peptides containing the -(Leu-Aib-Ala)$_2$-Phe-Aib-fragment. *Protein Sci.* **3**, 1547–1555.
58. Karle, I.L., Flippen-Anderson, J.L., Sukumar, M. & Balaram, P. (1988) Monoclinic polymorph of Boc-Trp-Ile-Ala-Aib-Ile-Val-Aib-Leu-Aib-Pro-OMe (anhydrous) parallel packing of 3_{10}-/α-helices and a transition of helix type. *Int. J. Pept. Protein Res.* **31**, 567–576.
59. Karle, I.L., Flippen-Anderson, J.L., Sukumar, M. & Balaram, P. (1990) Parallel and antiparallel aggregation of α-helices. *Int. J. Pept. Protein Res.* **35**, 518–526.